ORIGINAL ARTICLE

Systemic inflammatory and gut microbiota responses to fracture in young and middle-aged mice

Joseph L. Roberts · **Brandon Chiedo** ·
Hicham Drissi

Abstract Age is a patient-specific factor that can significantly delay fracture healing and exacerbate systemic sequelae during convalescence. The basis for this difference in healing rates is not well-understood, but heightened inflammation has been suggested to be a significant contributor. In this study, we investigated the systemic cytokine and intestinal microbiome response to closed femur fracture in 3-month-old (young adult) and 15-month-old (middle-aged) female wild-type mice. Middle-aged mice had a serum cytokine profile that was distinct from young mice at days 10, 14, and 18 post-fracture. This was characterized by increased concentrations of IL-17a, IL-10, IL-6, MCP-1, EPO, and TNFα. We also observed changes in the community structure of the gut microbiota in both young and middle-aged mice that was evident as early as day 3 post-fracture. This included an Enterobacteriaceae bloom at day 3 post-fracture in middle-aged mice and an increase in the relative abundance of the *Muribaculum* genus. Moreover, we observed an increase in the relative abundance of the health-promoting *Bifidobacterium* genus in young mice after fracture that did not occur in middle-aged mice. There were significant correlations between serum cytokines and specific genera, including a negative correlation between *Bifidobacterium* and the highly induced cytokine IL-17a. Our study demonstrates that aging exacerbates the inflammatory response to fracture leading to high levels of pro-inflammatory cytokines and disruption of the intestinal microbiota.

J. L. Roberts · H. Drissi
Department of Orthopaedics, Emory University School of Medicine, 21 Ortho Ln, 6th Fl, Office 12, Atlanta, GA 30329, USA

J. L. Roberts · B. Chiedo · H. Drissi (✉)
The Atlanta Department of Veterans Affairs Medical Center, Decatur, GA, USA
e-mail: hicham.drissi@emory.edu

J. L. Roberts (✉)
College of Health Solutions, Arizona State University, 850 N 5th St, Office 360J, Phoenix, AZ 85004, USA
e-mail: joseph.roberts.3@asu.edu

Introduction

Fractures are common events, especially in the elderly that have a residual life-time fracture risk of 29% in males and 56% in females [1]. Increased age is also a well-established risk factor for delayed fracture repair by impacting numerous steps of the healing process [2–4]. This delay has been attributed to several factors, including decreased responsiveness of mesenchymal progenitor cells to growth and differentiation

factors, an overall decrease in osteochondral progenitor cell numbers, diminished propensity for cell division and maturation of mesenchymal cells, and delayed callus vascularization [5]. Most fractures heal through secondary bone repair that involves an intricate series of overlapping stages that is initiated by a robust local and systemic inflammatory response [6]. This reactive inflammatory phase is critical to the progression of healing by facilitating the migration and differentiation of mesenchymal progenitor cells from the periosteum and bone marrow to the site of injury [6].

The function of the immune system changes with increasing age, which is often referred to as immunosenescence [7]. Age is also associated with increased levels of circulating inflammatory cytokines such as TNFα and IL-6, even in the absence of trauma [8, 9]. This excessive basal low-grade inflammation can contribute to a prolonged inflammatory phase that is detrimental to the progression of fracture healing [10, 11]. Immune cells from aged mice also display an enhanced pro-inflammatory response to bacteria and bacterial-derived products (e.g., lipopolysaccharide) [12]. This is important due to the age-driven increase in intestinal permeability that allows the paracellular translocation of microbial products to enter the bloodstream and promote inflammation [12]. Moreover, we recently demonstrated that simple femur fracture rapidly disrupts the intestinal barrier and alters the composition of the gut microbiota [13, 14]. However, little data exist concerning the interplay between the systemic inflammatory response to fractures and the gut microbiota in the context of aging [15, 16].

The gut microbiota is composed of a diverse group of bacteria that remains relatively stable in adults but undergoes dramatic changes with advanced age [17]. Microbial dysbiosis, or imbalance in the composition of the gut microbiota, occurs with age and these changes are sufficient to promote age-associated inflammation [12]. This was further supported by studies using young germ-free mice colonized with an aged microbiota that displayed enhanced T cell differentiation (CD4+ Th2, Th1, and Treg cells) and local inflammation within the intestine [18]. As such, the gut microbiota has emerged as a significant regulator of systemic inflammation and more recently been implicated in the maintenance and repair of the skeleton [13, 14, 19]. This study sought to characterize the differential systemic immune and gut microbiome response to femoral fracture between young and middle-aged mice. Herein, we demonstrate that the systemic inflammatory profile is distinct between young and middle-aged mice during the post-fracture period. Moreover, we highlight unique responses of the gut microbiota to femoral fracture in young and middle-aged mice.

Methods

Animal husbandry

Three-month-old C57BL/6J (Strain #000664) female mice were obtained from Jackson Laboratories and allowed to acclimate to the vivarium for 2 weeks prior to the start of all experiments. A separate cohort of 3-month-old female C57BL/6J mice were purchased from Jackson Laboratories and housed in the animal facility until 15 months of age. We elected to examine female mice in this study due to slower rate of fracture healing as well as clinical evidence showing that women may have an increased risk for fractures and atrophic non-unions compared to males [20]. Mice had *ab libitum* access to autoclaved food (Envigo #2018S) and water (0.1 micron filtered). All mice were group housed at the Atlanta Veterans Affairs Medical Center (VAMC) vivarium in specific pathogen-free cages, with sterilized corn cob bedding, and controlled conditions (temperature, 21–24 °C; humidity, 40–70%; light/dark cycle, 12/12 h). Mice were weighed prior to fracture and at days 3, 7, 10, 14, and 18 post-fracture. Changes in body weight are presented as percent change from baseline (prior to fracture). Mice were maintained in accordance with applicable state and federal guidelines and all experimental procedures were approved by the Atlanta VAMC Institutional Animal Care and Use Committee.

Fracture model

Femoral fractures were generated using the Einhorn method and as we have previously described [21–23]. Three-month-old (young) and 15-month-old (middle-aged) mice were anesthetized with isoflurane inhalation and administered analgesics (Buprenorphine SR), and the left hind limb was shaved and sterilized

with chlorohexidine and isopropyl alcohol. The articular surface of the femoral intercondylar notch was then perforated with a 25-gauge needle through the skin, followed by insertion of a precut stainless steel 316LVM wire (small part diameter 0.15 inch) into the medullary canal with the use of a retrograde approach. A transverse mid-diaphyseal fracture was then created using three-point bending via a blunt guillotine device. The fractured limbs were radiographically examined by digital X-ray (Bruker) immediately post-fracture to confirm fracture location and pin placement. Animals with comminuted, distal, or proximal fractures were excluded from the histological and micro-computed tomography (μCT) studies. Mice were allowed to fully weight-bear without any restrictions on activity after recovery from anesthesia. At either 10, 14, or 18 days post-fracture, mice were euthanized by CO_2 asphyxiation followed by cervical dislocation. These timepoints were selected as they represent critical events during fracture healing, corresponding to callus vascularization (day 10), the cartilaginous-to-bony callus transition (day 14), and initiation of callus remodeling (day 18).

Micro-computed tomography

μCT was performed on the fractured femur to determine callus bone using a μCT40 scanner (Scanco Medical AG, Brüttisellen, Switzerland) that was calibrated weekly using a factory-supplied phantom (day 14: $n = 5$/group; day 18: $n = 4$/group). Bones were first fixed for 1 week in 10% neutral buffered formalin at 4 °C followed by scanning in PBS medium. For fracture callus analyses, fracture calluses were manually segmented to exclude existing cortical bone and any bone fragments at the center of the fracture callus. A Gaussian filter (sigma = 0.8, support = 1) was applied to reduce noise, and the following measures of callus structure and composition were quantified for each fracture callus: total callus volume (TV), mineralized callus volume (BV), and bone volume fraction (BV/TV).

Gene expression

An approximately 1-cm section of the small intestines ($n = 5$/group) corresponding to the duodenum was collected, flash frozen, and stored at − 80 °C until analysis. The frozen small intestine was homogenized using a tissue grinder and total RNA was isolated using TRIzol (Invitrogen). First-strand cDNA was synthesized with oligo(dT) and random primers using qScript cDNA SuperMix (Quantabio). All qRT-PCR were performed on an Analytik Jena qTower^3 G Real-Time PCR Detection System using PerfeCTa SYBR Green FastMix (Quantabio). Amplicon authenticity was confirmed by melt curve analysis. Expression of genes encoding tight junction proteins (*Ocln*, *Jam3*, *Cldn2*, *Tjp1*), the major component of the protective mucus layer (*Muc2*), and biomarker of intestinal dysbiosis and inflammation (*Lcn2*) were quantified. Primer sequences are provided in Supplementary Table 1 and β-actin was used as the normalization control. The data were analyzed using the $\Delta\Delta$CT method.

Measurement of serum cytokines

Whole blood was obtained by cardiac puncture at time of harvest ($n = 5$/group/timepoint), allowed to clot at room temperature for $\geq$ 30 min, then centrifuged at $10,000 \times g$ for 10 min. Serum was then removed, aliquoted, and stored at − 80 °C. Systemic cytokines were assayed using a Meso Scale Discovery U-Plex electrochemiluminescence assay for a total of 20 cytokines according to manufacturer's instructions at the Emory Multiplex Immunoassay Core. The investigated markers were EPO, GM-CSF, IFN-γ, IL-1β, IL-4, IL-6, IL-10, IL-13, IL-16, IL-17a, IL-17c, IL-17e/IL-25, IL-17f, IL-21, IL-22, IL-23, IL-33, MCP-1, TNFα, and VEGF-a. Lower limits of quantification (LLOQ) were as follows: EPO: 3.78 pg/ml; GM-CSF: 0.0629 pg/ml; IFN-γ: 0.0626 pg/ml; IL-10: 1.55 pg/ml; IL-13: 2.52 pg/ml; IL-16: 1.38 pg/ml; IL-17a: 0.0977 pg/ml; IL-1β: 1.11 pg/ml; IL-4: 0.175 pg/ml; IL-6: 1.86 pg/ml; IL-17c: 0.789 pg/ml; IL-17e: 0.335 pg/ml; IL-17f: 21.1 pg/ml; IL-21: 1.26 pg/ml; IL-22: 0.356 pg/ml; IL-23: 1.36 pg/ml; IL-33: 0.755 pg/ml; MCP-1: 1.69 pg/ml; TNFα: 1.69 pg/ml; and VEGF-a: 0.431 pg/ml. Undetectable concentrations of any cytokine were recorded as one-half of the lower limit of quantification, with the exception of GM-CSF, IL-13, IL-4, IL-17c, IL-17e/IL-25, IL-17f, and IL-1β (day 10) which were not detected in any sample and were excluded from analyses.

Fecal metagenomic sequencing

Fecal pellets (~ 50 mg) were longitudinally collected from mice ($n = 4$/group/timepoint) in sterile microcentrifuge tubes, placed in dry ice, and stored at − 80 °C until analysis. DNA extraction, sequencing, and bioinformatics were completed by Microbiome Insights (Vancouver, Canada). Briefly, fecal DNA was extracted using the Qiagen MagAttract PowerSoil DNA KF kit using a KingFisher robot. DNA quality was evaluated visually via gel electrophoresis and quantified using a Qubit 3.0 fluorometer (Thermo Fisher). Libraries were prepared using an Illumina Nextera library preparation kit with an in-house protocol (Illumina). Paired-end sequencing (150 bp × 2) was completed on a NextSeq 500 in medium-output mode. Shotgun metagenomic sequence reads were processed with the Sunbeam pipeline. Initial quality evaluation was completed using FastQC v0.11.5. Processing took part in four steps: adapter removal, read trimming, low-complexity-read removal, and host-sequence removals. Adapter removal was done using cutadapt v2.6. Trimming was done with Trimmomatic v0.36 using custom parameters (LEADING:3 TRAILING:3 SLIDINGWINDOW:4:15 MINLEN:36). Low-complexity sequences were detected with Komplexity v0.3.6. High-quality reads were mapped to the human genome (Genome Reference Consortium Human Reference [24]) and the mouse *Mus musculus* (house mouse) genome assembly GRCm38.p6, and those that were mapped to it with at least 50% similarity across 60% of the read length were removed. The remaining reads were taxonomically classified using Kraken2 with the PlusPF database from 17 May 2021. For functional profiling, filtered reads were aligned against the SEED database via translated homology search and annotated to subsystems (functional levels) 1–3 using Super-Focus with level 1 being the most general and level 3 being the most specific. Three of the middle-aged samples ($n = 1$ at days 3, 14, 18) were removed from data analysis because of high host contamination (> 25%).

Statistical and bioinformatic analysis

Results are shown as mean ± SD. Statistical significance was determined by either unpaired two-tailed Student's *t*-test, mixed-effects model for repeated measures followed by Tukey's multiple comparisons as appropriate, Scheirer-Ray-Hare test for the two-factor analysis, or two-way ANOVA with Sidak post hoc testing as indicated in the figure legends using GraphPad Prism software (version 9.5.1). All statistical tests were performed at the 5% significance level. Outliers were identified using the ROUT method ($Q = 1\%$) and were removed from datasets when appropriate. Prior to principal component analysis (PCA) and heat map generation, serum cytokine concentrations were log-transformed then converted to *Z*-scores. PCA of serum cytokine data was carried out as an exploratory data analysis tool using JMP Pro 16 (SAS). Each dot represents a sample projected onto the two main principal components and the color of the dot represents the age of mice. Pearson's correlation test was utilized for correlation analyses comparing serum cytokines and the top ten most abundant genera at day 18 post-fracture. Microbial alpha diversity was estimated using the Shannon diversity index on raw OTU abundances. Beta diversity was estimated using OTUs to compute the Bray-Curtis indices. Beta diversity was visualized using principal coordinates analysis of ordination (PCoA) and variation in community structure was assessed with permutational multivariate analyses of variance (PERMANOVA). Negative binomial models (DESEq2 R package) were used for differential abundance testing of taxonomic and function subsystem level 3 features to examine differences between ages across timepoints (timepoint to age interaction). *P*-values were calculated with LRT test with an adjusted *P*-value = 0.01. Taxa and functions that were present in less than 10% of the samples were excluded to reduce false positives. All microbiome analyses were conducted in the R environment by Microbiome Insights (Vancouver, Canada).

Results

Fracture healing is delayed in middle-aged mice

Young (3-month-old) and middle-aged (15-month-old) female C57BL/6J mice were subjected to unilateral femoral fractures and were used to assess fracture healing, systemic cytokines, and fecal microbiome changes (Fig. 1A). Femur fracture induced a rapid decrease in body weight in both young (− 4%) and middle-aged (− 13%) mice
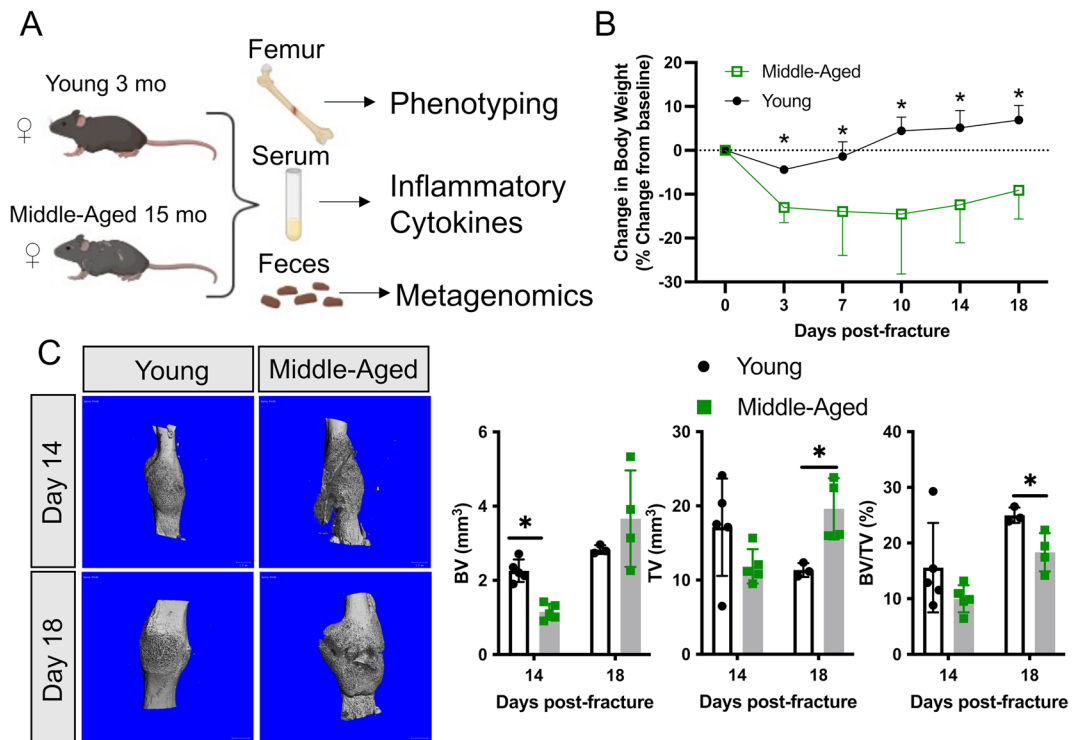
Fig. 1 Middle-aged mice experience a delay in secondary bone repair. **A** Young 3-month-old and middle-aged 15-month-old female wild-type mice were used to assess the systemic inflammatory cytokine and gut microbiome response to fracture. **B** Fracture leads to a rapid and sustained decrease in body weight in middle-aged mice. **C** MicroCT 3D reconstruction of fracture calluses at day 14 ($n = 5$/group) and 18 ($n = 4$/group) post-fracture shows differences in callus mineralization between young and middle-aged mice. At day 14 post-fracture, there was significantly less bone volume in middle-aged mice. At day 18 post-fracture, the callus size was significantly larger and contained less bone in middle-aged mice. Data represent mean ± SD. Student's unpaired t-test, $*P < 0.05$ vs. young mice

within the first 3 days; however, this decrease was significantly greater in middle-aged mice (Fig. 1B). Moreover, the young mice recovered from this initial loss in body weight by 1-week post-fracture and continued to accrue body weight throughout healing, but the middle-aged mice never recovered to their pre-fracture weight (Fig. 1B).

Assessment of fracture healing by microCT revealed a significant decrease in callus bone volume (BV, − 49%) at day 14 post-fracture in the middle-aged mice (Fig. 1C). At day 18 post-fracture, the differences between young and middle-aged mice were more evident by microCT volumetric analyses, in which the middle-aged mice had significantly larger calluses (TV, + 73%) that contained less bone (BV/TV, − 27%) (Fig. 1C). Together, these data indicate that 15-month-old mice are a valid healing-challenged model.

Middle-aged mice have an exacerbated systemic inflammatory response to fracture

We next sought to determine if the systemic inflammatory response was altered in middle-aged mice. PCA of serum cytokines revealed that the inflammatory response to fracture was distinct between young and middle-aged mice at days 10, 14, and 18 post-fracture (Fig. 2A, B). There was a significant effect of age on MCP-1, TNFα, EPO, IL-17a, IL-6, IL-10, IFNγ, and IL-16 concentrations and a significant effect of time on EPO, IL-10, IL-17a, TNFα, IFNγ, VEGFa, IL-33, GM-CSF, IL-1β, and IL-22 (Fig. 2C and Supplementary Fig. 1). Moreover, there was a significant interaction effect for IL-17a (Fig. 2C). MCP-1 and TNFα were significantly higher in middle-aged mice at all timepoints. At day 14 post-fracture, serum IL-6 and IL-10 were
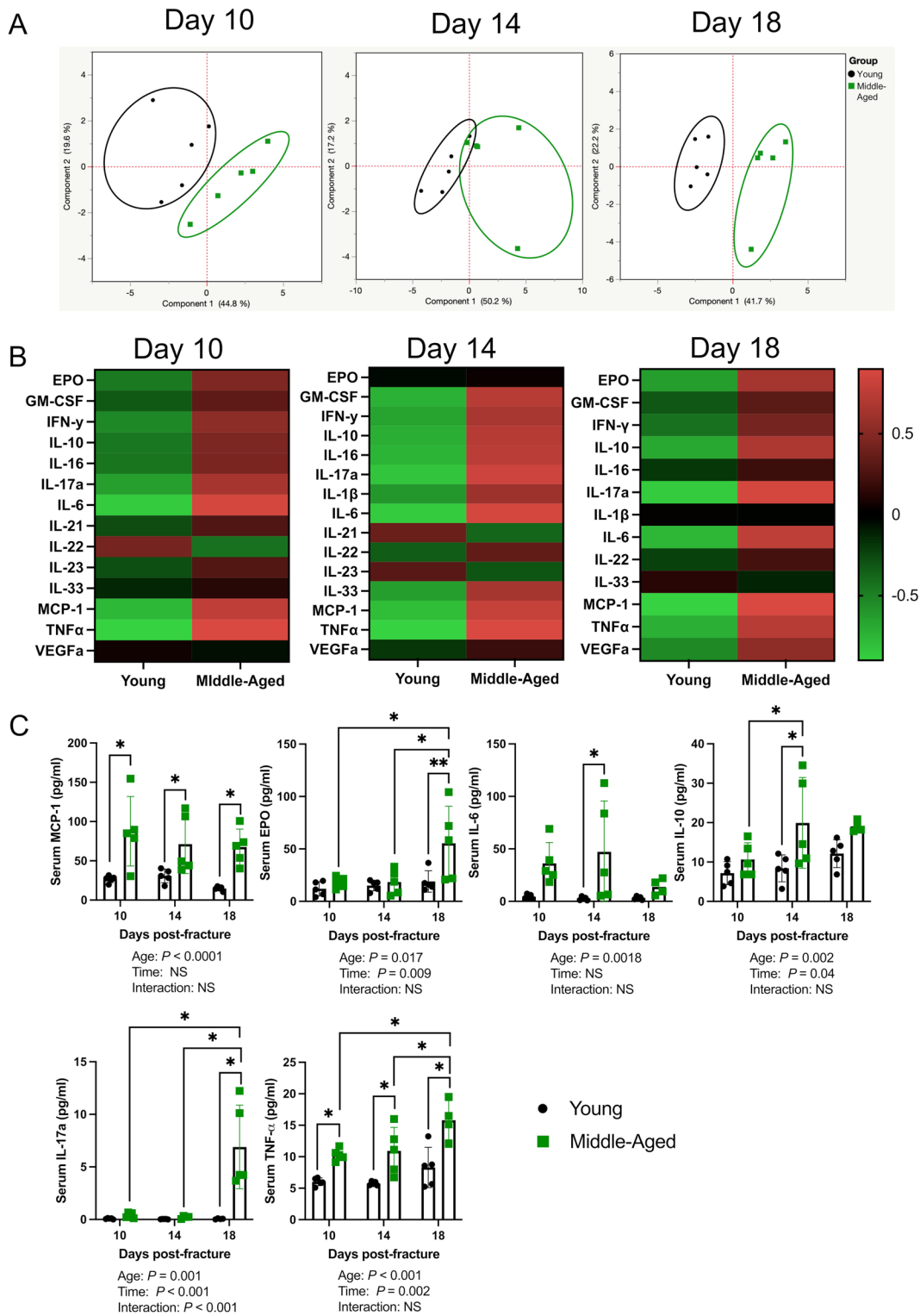
◄**Fig. 2** Middle-aged mice have a distinct inflammatory response to fracture. **A** Principal component analyses of serum cytokines show a clear distinction between young and middle-aged mice at days 10, 14, and 18 post-fracture (n = 5/group/timepoint). **B** Heat map depicting group averages of serum cytokines. **C** There was a significant effect of age on MCP-1, TNFα, EPO, IL-17a, IL-6, and IL-10 concentrations and a significant effect of time on EPO, IL-10, IL-17a, and TNFα. Outliers were identified the middle-aged dataset using the ROUT method in day 18 IL-6 (excluded value 63.34 pg/ml), day 18 IL-10 (excluded value 45.91 pg/ml), day 18 TNFα (excluded value 37.5 pg/ml), and day 14 IL-17a (excluded value 3.85 pg/ml). Data represent mean ± SD. Two-way ANOVA followed by Sidak's multiple comparisons test, *P < 0.05

significantly higher in middle-aged mice, whereas at day 18 post-fracture, serum IL-17a and EPO were significantly higher in middle-aged mice compared to young mice. At day 18 post-fracture, there was also a significant increase in the concentrations of EPO, TNFα, IL-17a, and VEGFa when compared to days 10 and 14 post-fracture in middle-aged mice, which was not observed in young mice (Fig. 2C and Supplementary Fig. 1). In young mice, there was a significant increase in IL-33, GM-CSF, and IFNγ at day 18 post-fracture compared to days 10 and 14, while the concentration of IL-22 decreased from days 10 to 14 post-fracture in young mice (Supplementary Fig. 1).

Middle-aged mice have differential expression of intestinal tight junction-related genes

We next measured the expression of genes that code for proteins involved in formation of tight junctions between adjacent epithelial cells within the small intestines of young and middle-aged mice at day 18 post-fracture, a timepoint when callus mineralization was significantly different between ages (Fig. 1C). The expression of occludin (*Ocln*), ZO-1 (*Tjp1*), and claudin-2 (*Cldn2*) was significantly lower in middle-aged mice compared to young mice (Fig. 3). The expression of *Jam3* and mucin-2 (*Muc2*) was not significantly different between ages (Fig. 3). Moreover, the expression of lipocalin-2 (*Lcn2*) that is induced during dysbiosis [25] was significantly higher (+ 123%) in middle-aged mice (Fig. 3). Together, these data suggest that middle-aged mice have a compromised intestinal barrier.

Femoral fracture alters the composition of the gut microbiome

Metagenomic sequencing of longitudinally collected fecal samples revealed that in young mice across all timepoints, bacteria dominated the communities followed by eukaryotes, archaea, and viruses accounting for 99.62%, 0.22%, 0.14%, and 0.02%, respectively (Supplementary Figure 2). In middle-aged mice, bacteria also dominated the communities followed by eukaryotes, archaea, and viruses accounting for 99.04%, 0.68%, 0.23%, and 0.05% respectively across all timepoints (Supplementary Figure 2). There was a significant effect of age on the abundance of bacteria, eukaryotes, archaea, and viruses (Supplementary Figure 2). There was also a significant interaction between age and timepoint for viruses, with middle-aged mice having an increased relative abundance of viruses prior to fracture and at days 10, 14, and 18 post-fracture (Supplementary Figure 2). As expected, there was a baseline difference (prior to fracture) in the beta diversity between young and middle-aged mice (Fig. 4A). Alpha diversity, calculated using the Shannon diversity index, was significantly different between ages while time and the interaction between time and age were not significant (Fig. 4B). Moreover, the middle-aged mice displayed significantly higher alpha diversity prior to fracture and at days 3, 10, and 18 post-fracture compared to young mice (Fig. 4B). At day 14 post-fracture, there were no significant differences in alpha diversity between ages (Fig. 4B). Analysis of overall microbial community composition changes throughout fracture healing by PERMANOVA revealed a significant effect of age (P = 0.001, R^2 = 0.389), timepoint (P = 0.047, R^2 = 0.041), and age to timepoint interaction (P = 0.022, R^2 = 0.051) (Fig. 4B). Several indexes have been developed to assess intestinal microbiota imbalances, primarily in the context of metabolic disease [26]. No significant differences in the Firmicutes/Bacteroidetes (F/B) ratio were identified between ages or across time (Fig. 4C). Middle-aged mice, however, displayed a significant increase in the *Prevotella*/Bacteroidetes prior to fracture and at all post-fracture timepoints (Fig. 4D). We further examined the relative abundance of the Enterobacteriaceae family, which is linked to inflammation, and observed a significant bloom in Enterobacteriaceae in the middle-aged mice compared to young mice at day
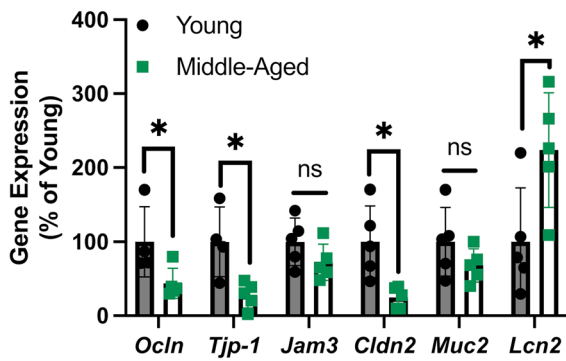
Fig. 3 Middle-aged mice have gut barrier defects. Middle-aged mice displayed decreased expression of occludin (*Ocln*), ZO-1 (*Tjp1*), and claudin-2 (*Cldn2*) and increased expression of lipocalin-2 (*Lcn2*) in the small intestine at day 18 post-fracture. Outliers were identified the young dataset using the ROUT method for *Ocln* (n = 1) and *Tjp1* (n = 1). Data represent mean ± SD (n = 4–5/group). Student's unpaired *t*-test, *P < 0.05 vs. young mice

3 post-fracture (Fig. 4E). Together, these data indicate that middle-aged mice have a baseline level of dysbiosis which can be exacerbated by femoral fracture.

The taxonomic composition at the genus level displayed marked changes that persisted throughout the course of fracture healing in young and middle-aged mice (Fig. 5A). In young mice, there was an increase in the relative abundance of *Bifidobacterium* at days 10 and 14 post-fracture compared to pre-fracture levels (Fig. 5B). The change in the abundance of *Bifidobacterium* was not observed in middle-aged mice (Fig. 5B). Fracture also led to a significant decrease in the abundance of *Lactobacillus* in young mice at days 10, 14, and 18 post-fracture compared to pre-fracture levels, which was not observed in middle-aged mice (Fig. 5B). Moreover, there was a significant expansion of *Muribaculum* and decreased *Ligilactobacillus* at day 3 post-fracture in middle-aged mice (Fig. 5B). The abundance of *Ligilactobacillus* and *Muribaculum* did not change in young mice. At the species level, similar disturbances in the top 10 must abundant species were observed after femoral fracture in young and middle-aged mice (Fig. 5C). Differential abundance testing (DESEq2) for differences between
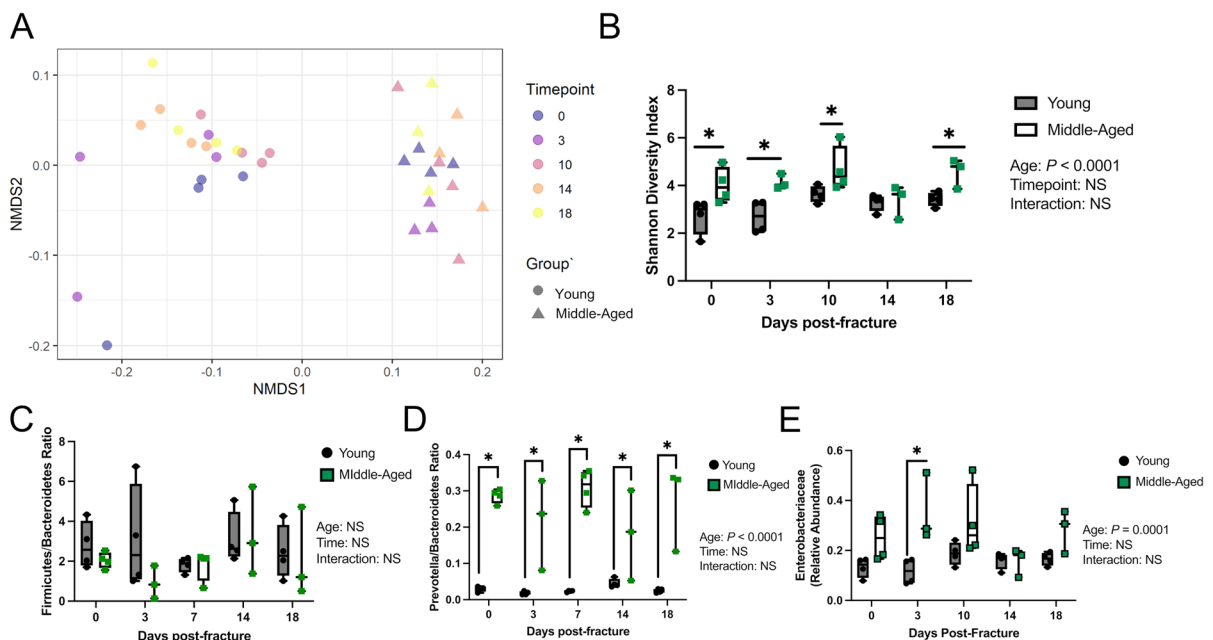

Fig. 4 Middle-aged mice experience dysbiosis. **A** Principal coordinates ordination analyses (PCoA) of fecal beta diversity (n = 3–4/group/timepoint). **B** Middle-aged mice have significantly higher fecal alpha diversity compared to young mice at all timepoints except day 14 post-fracture. **C** No difference in the Firmicutes/Bacteroidetes ratio between ages, timepoints, and age to timepoint interaction. **D** Middle-aged mice had significantly higher *Prevotella*/Bacteroidetes ratios at each timepoint. **E** At day 3 post-fracture, there was a significant increase in Enterobacteriaceae in middle-aged mice compared to young mice. Two-way ANOVA followed by multiple comparisons testing, *P < 0.05 vs. young mice
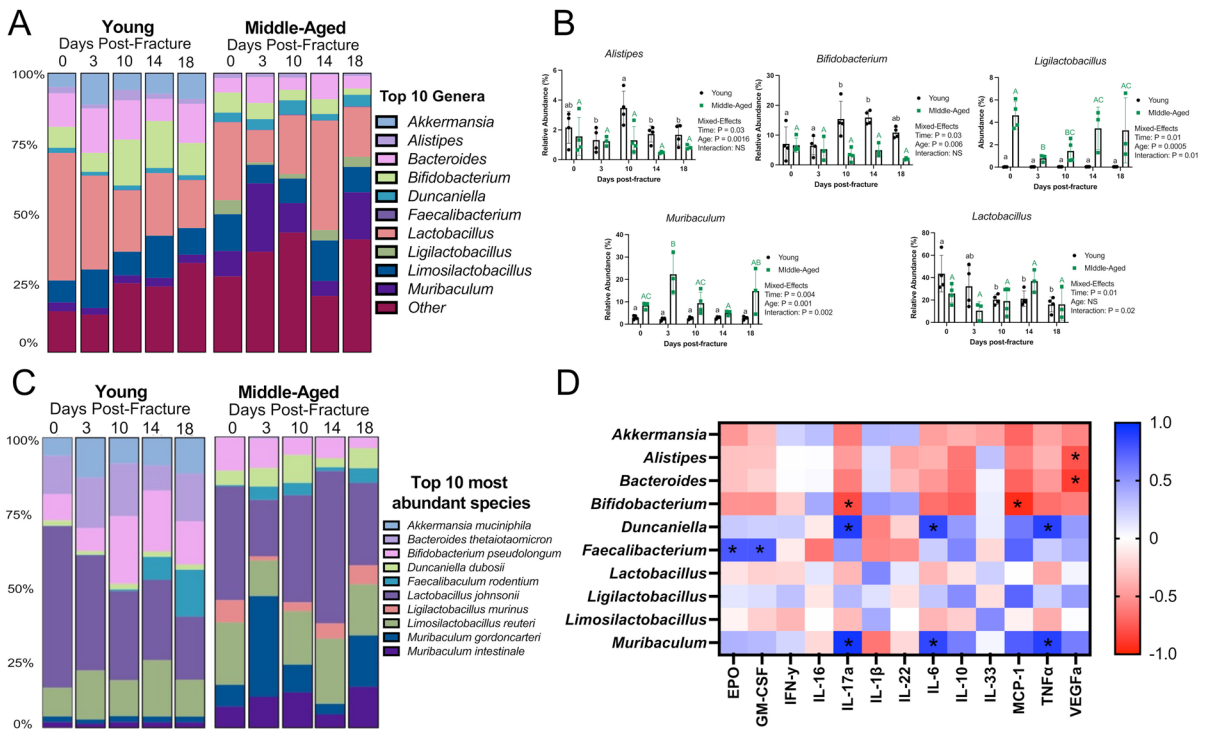
Fig. 5 Fracture alters the composition of the gut microbiota. **A** Detailed relative abundance of bacteria showing changes in the top 10 most abundant genera prior to fracture (day 0) and at days 3, 10, 14, and 18 post-fracture. **B** Changes in the relative abundances of specific genera throughout fracture healing. Values of the same color and case not sharing a common letter are significantly different, *P* < 0.05 (*n* = 3–4/group/timepoint). Data were assessed using a mixed-effects model followed by Tukey's multiple comparison testing. **C** Detailed relative abundance of bacteria showing changes in the top 10 most abundant species prior to fracture (day 0) and at days 3, 10, 14, and 18 post-fracture. **D** Pearson correlation matrix heat map showing relationships between serum cytokine levels and the relative abundance of the top 10 most abundant genera at day 18 post-fracture, *P* < 0.05

ages across timepoints (age to timepoint interaction) identified 73 significant taxa (Supplementary Table 2).

To determine if the relative abundance of the top 10 genera were related to serum cytokines, heat maps were created based on Pearson's correlation coefficient (*r*) using day 18 samples. This timepoint was selected for this analysis because the serum cytokines and fecal samples were obtained from the same animals. *Bifidobacterium* was negatively correlated with IL-17a and MCP-1 levels. *Alistipes* and *Bacteroides* were negatively correlated with VEGFa. *Duncaniella* and *Muribaculum* were positively correlated with IL-17a, IL-6, and TNFα. *Faecalibacterium* was positively correlated with EPO and GM-CSF. Our results suggest that changes in the cytokine profile after fracture are closely correlated with alterations in the abundance of the fecal microbiota.

Femoral fracture does not markedly alter the metagenomic functional profile

Analysis of overall functional profile changes throughout fracture healing by PERMANOVA revealed a significant effect of age (*P* = 0.001, R^2 = 0.180). There were no significant differences in functional profiles due to timepoint (*P* = 0.057, R^2 = 0.058) or interaction between age and timepoint (*P* = 0.079, R^2 = 0.05). Differences in functional profiles between young and middle-aged mice were present prior to fracture (*P* = 0.044, R^2 = 0.384) and day 14 post-fracture (*P* = 0.031, R^2 = 0.386) (Fig. 6A). Differential abundance testing for differences between ages across timepoints (age to timepoint interaction) identified 17 significant functions of subsystem level 3 SEED features (Supplementary Table 3). The majority of (5 of 17) differentially abundant functions
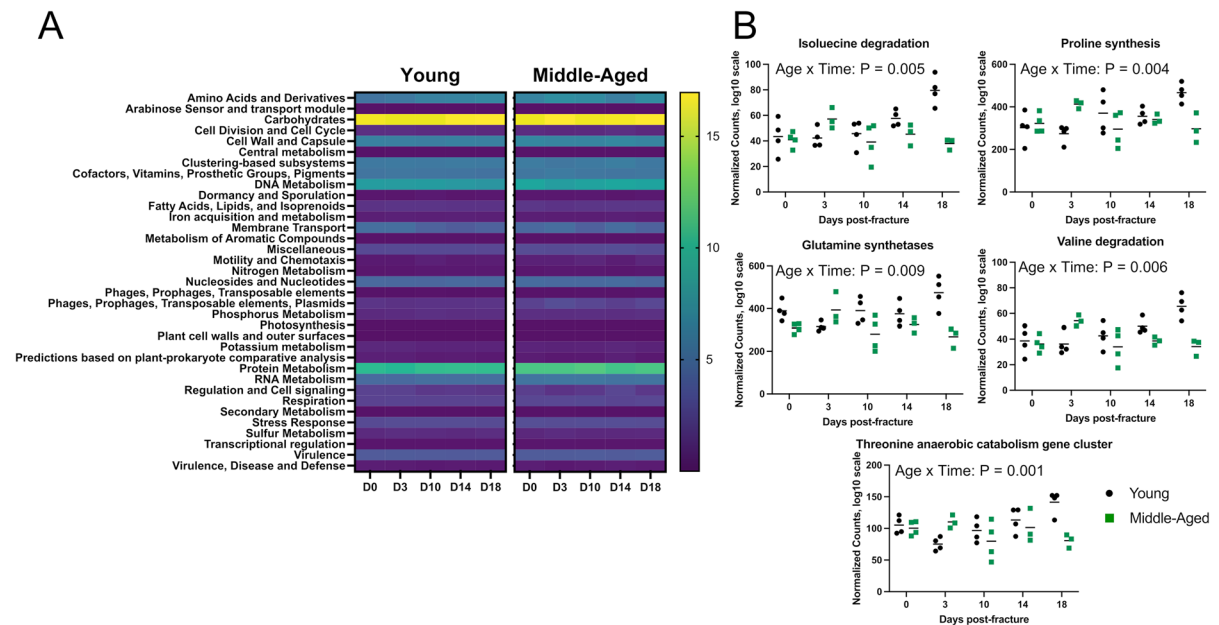
Fig. 6 Changes in functional profiles after fracture. **A** Heat map showing SEED subsystem level 1 functional profiles prior to fracture (day 0) and at days 3, 10, 14, and 18 post-fracture. **B** Differential abundance testing of SEED subsystem level 3 functions revealed that functions related to amino acid metabolism were different between groups across timepoints, ($n = 3$–4/group/timepoint)

involved amino acid metabolism, including threonine anaerobic catabolism gene cluster, proline synthesis, isoleucine degradation, valine degradation, and glutamine synthetases (Fig. 6B).

Discussion

Increased age is associated with a number of pathologies and comorbidities. This includes an overall increased risk of fracture as well as a higher likelihood of experiencing complications during healing [2, 27–29]. Geriatric fracture healing is also associated with more negative systemic complications than those of younger patients. The heightened inflammatory response that occurs in aging likely contributes to this phenomenon. In our study, we observed a large initial ($-$13%), yet sustained loss of body weight in middle-aged mice. Traumatic injuries, including fracture, induce an initial suppression in appetite before entering into a hypermetabolic state [30, 31]. For instance, a well-nourished patient with a fracture can experience a 20–25% increase in metabolic rate [32]. This hypermetabolism is partly driven

by the inflammatory reaction to injury, which was exacerbated in the middle-aged mice [31]. The sustained decrease in body weight may contribute to the impaired fracture healing phenotype as the period of rapid bone formation during healing is metabolically expensive. Although we did not directly address energy expenditure in these mice, our data point to inflammation as a contributor to the weight loss in middle-aged mice which could be further addressed in future studies.

Aging has been shown to delay fracture healing, with aged mice having larger fracture calluses that contain less bone [2, 33, 34]. Our study demonstrating delayed healing in 15-month-old mice is in agreement with these previous reports. The systemic drivers that underpin this delay in fracture healing are not well-defined. It is established that aged mice have a basal pro-inflammatory state that is characterized by higher levels of the proinflammatory cytokines [28]. The systemic inflammatory response to injury and fracture is also exacerbated in aged mice [16, 24, 33, 35]. These prior studies support our findings of a distinct systemic inflammatory cytokine profile in middle-aged mice during fracture healing.

The middle-aged mice in our study had significantly higher levels of several pro-inflammatory cytokines after fracture, including IL-17a, IL-10, IL-6, MCP-1, and TNFα. The high levels of inflammatory cytokines may have impaired the natural progression of secondary bone healing, therefore delaying healing in the middle-aged mice. In fact, high concentrations of TNFα can not only impair fracture healing [36–38] but also impair angiogenesis [39]. Increased IL-6 has also been associated with unfavorable outcomes [40, 41]. Heightened levels of these cytokines may contribute to the delayed fracture healing observed in middle-aged mice.

IL-17a was the only cytokine with a significant interaction effect between time and age. Moreover, it was the most strongly increased cytokine in the middle-aged mice at days 10 (+ 485%), 14 (+ 2367%), and 18 (+ 10408%) post-fracture compared to young mice. Similarly, IL-17a was reported to be strongly induced after bone injury where it promoted osteoblastogenesis of injury-associated mesenchymal cells [42]. Conversely, inhibiting IL-17a *in vivo* by injecting an IL-17a blocking antibody improved intramembranous ossification in a drill hole model of bone regeneration [43]. Thus, the influence of IL-17a on osteogenesis is controversial, with no clear consensus of its effects on osteogenic differentiation. Some studies classify IL-17a as a pro-osteogenic effector [42, 44–48], whereas others report either no effect [49] or repression of osteogenesis [42, 50–54]. Additional studies are ultimately warranted to fully interrogate the influence of IL-17a on fracture healing in the context of aging.

We and others have reported that age and simple femoral fractures can promote intestinal dysfunction characterized by a rapid disruption of the intestinal barrier [12–14, 55]. Increased gut permeability can increase systemic inflammation due to the paracellular translocation of microbial-derived antigens that can reach distal sites [55]. In our study, we observed decreased expression of genes (*Ocln*, *Tjp1*, *Cldn2*) involved in the formation of tight junctions within the small intestine in middle-aged mice at day 18 post-fracture. We also observed a significant increase in the gene expression of lipocalin-2 (*Lcn2*) within the small intestine in middle-aged mice. *Lcn2* expression is strongly induced by endotoxin, and it has been identified as an indicator of intestinal inflammation [56, 57]. Moreover, dysbiosis can induce lipocalin-2

expression, which functions to limit bacterial growth by sequestering iron [58].

There is an increasing number of studies that have identified characteristic alterations in the gut microbiota in the elderly that are associated with health outcomes [59–64]. We also identified marked taxonomic differences in the microbiomes of young and middle-aged mice prior to fracture. Interestingly, we observed increased alpha diversity in middle-aged mice prior to fracture and throughout fracture healing, with the exception of day 14 post-fracture. The Shannon index of alpha diversity is a measure of within-sample diversity accounting for both species richness (i.e., number of species) and evenness (i.e., distribution). While increased diversity is largely considered to be beneficial, several studies have reported increased alpha diversity in aging [17, 65, 66]. Importantly, our results highlight a stability in alpha diversity in young mice, which fluctuated in middle-aged mice after fracture. We also observed an increase in the Enterobacteriaceae family at day 3 post-fracture in middle-aged mice compared to young mice. Many members of the Enterobacteriaceae family are facultative anaerobic bacteria with pathogenic properties [67]. These bacteria contain immunostimulatory microbe-associated molecular patterns, such as lipopolysaccharides, that have been linked to enhanced inflammatory responses [68]. The bloom of potentially pathogenic Enterobacteriaceae family may have contributed to the heightened post-fracture systemic inflammation response observed in middle-aged mice.

In our study, fracture led to unique perturbations in bacterial communities in both young and middle-aged mice. There was an expansion of the beneficial *Bifidobacterium* genus in young mice after fracture that was not observed in middle-aged mice, whereas the abundance of the *Lactobacillus* genus decreased after fracture in young mice. *Bifidobacterium* and *Lactobacillus* are both lactic acid bacteria that utilize similar substrates [69]. The fracture-induced expansion of *Bifidobacterium* in young mice may have contributed to the decreased abundance of *Lactobacillus*. Alternatively, the decrease in *Lactobacillus* may have opened ecological niches that permitted the expansion of *Bifidobacterium*. Bacteria belonging to the *Bifidobacterium* and *Lactobacillus* genera are common probiotics and have received considerable attention for their health-promoting properties in a variety of disease

states, including bone health [70]. We recently published that supplementing aged mice (18-month-old) with *Bifidobacterium longum* accelerated and enhanced fracture healing [13]. We also reported a beneficial effect of *Bifidobacterium adolescentis* supplementation on fracture-related sequalae in young 3-month-old male mice [14]. In both studies, supplementing with species from the *Bifidobacterium* genus dampened systemic inflammation [13, 14]. The present study revealed a negative correlation between the relative abundance of the *Bifidobacterium* genus with IL-17a and MCP-1 levels at day 18 post-fracture, suggesting that *Bifidobacterium* may attenuate systemic inflammation after bone fracture. In agreement with our study, negative correlations between the abundance of *Bifidobacterium* and IL-17a levels have been reported in the context of various disease states [71–74]. Therefore, it is tempting to speculate that the expansion of *Bifidobacterium* during the reparative phase of secondary bone repair (days 10 and 14) in young mice may have contributed to the differences in callus mineralization and systemic inflammation. At day 3 post-fracture, there was also a significant decrease in the abundance of the *Ligilactobacillus* genus and increase in the *Muribaculum* genus in middle-aged mice but not in young mice. We observed similar effects in 18-month-old female mice at day 3 post-fracture [13]. *Muribaculum*, which belongs to the family Muribaculaceae previously known as S24-7, has been reported to rapidly bloom after liver injury and was correlated with inflammatory gene expression [75]. We also observed a positive correlation between *Muribaculum* and serum TNFα concentrations. TNFα is a potent pro-inflammatory cytokine that was identified as a central regulatory cytokine induced by aged microbiota in conventionally raised mice and germ-free mice colonized with an aged microbiota [18]. TNFα and the gut microbiota were also demonstrated to be critical for age-associated inflammation [12]. Future experimental studies are ultimately needed to decipher whether and how post-fracture fluctuations in these genera contribute to bone healing and the systemic inflammatory response to fracture.

Beyond the influence on immune system, the indigenous gut microbiota produce a wide repertoire of metabolites from dietary substrates that can influence host physiology, including short-chain fatty acids, secondary bile acids, and tryptophan metabolites. Prior studies have identified functional differences between young and aged microbiomes, including associations between amino acid metabolism and aging [59, 76]. While the functional profiles between young and middle-aged mice were similar in our study, we did identify several significant features. Approximately 30% (5 of 17) of the identified functions in with a significant age to timepoint interaction were related to amino acid metabolism. We do not know if these changes in metabolic features resulted in altered systemic metabolite levels. It is also unclear what effect, if any, these changes in microbial functional profiles have on fracture healing and systemic inflammation. Future studies will need to determine if alterations in the functional capacity of the middle-aged microbiota influence bone repair and post-fracture systemic inflammation.

This study is not without limitations. We utilized 15-month-old mice, which are generally considered upper middle-aged and not yet considered old. However, these mice exhibit a pro-inflammatory cytokine profile and delay in fracture healing that is consistent with aging. We would expect to find similar, if not more pronounced, differences in older animals (18–24 months old). Another limitation of the current study is that we did not assess basal cytokines prior to fracture or at a later timepoint when healing is complete. This limits our ability to determine if fracture was the primary driving force behind the heightened inflammation, or if the middle-aged mice had a basal level of inflammation that was already distinct from the young mice. It is conceivable that the middle-aged mice had elevated levels of cytokines prior to fracture that became more pronounced during the post-traumatic period [28]. We were also unable to examine the longitudinal relationships between systemic inflammation and the gut microbiota at all timepoints due to the terminal nature of blood collection. Future studies are needed to determine whether the observed longitudinal changes in bone healing and systemic inflammation in aging are due to enrichment of specific species, changes in microbiota interactions, or changes in the availability of microbiota-derived biomolecules.

In conclusion, we demonstrated that middle-aged mice have a distinct systemic inflammatory profile after fracture. This profile was characterized by high levels of the pro-inflammatory cytokine IL-17a. We also observed fracture-induced changes in

the composition of the gut microbiota that differed between young and middle-aged mice, which correlated to systemic cytokine levels. Importantly, this study adds new insight into the relationship between bone-gut axis in the context of aging.

Declarations

References

1. Jones G, Nguyen T, Sambrook PN, Kelly PJ, Gilbert C, Eisman JA. Symptomatic fracture incidence in elderly men and women: the Dubbo Osteoporosis Epidemiology Study (DOES). Osteoporos Int. 1994;4(5):277–82.

2. Naik AA, Xie C, Zuscik MJ, Kingsley P, Schwarz EM, Awad H, Guldberg R, Drissi H, Puzas JE, Boyce B, Zhang X, O'Keefe RJ. Reduced COX-2 expression in aged mice is associated with impaired fracture healing. J Bone Miner Res. 2009;24(2):251–64.

3. Lu C, Miclau T, Hu D, Hansen E, Tsui K, Puttlitz C, Marcucio RS. Cellular basis for age-related changes in fracture repair. J Orthop Res. 2005;23(6):1300–7.

4. He B, Zhang Z-K, Liu J, He Y-X, Tang T, Li J, Guo B-S, Lu A-P, Zhang B-T, Zhang G. Bioinformatics and microarray analysis of miRNAs in aged female mice model implied new molecular mechanisms for impaired fracture healing. Int J Mol Sci. 2016;17(8):1260.

5. Stolzing A, Jones E, McGonagle D, Scutt A. Age-related changes in human bone marrow-derived mesenchymal stem cells: consequences for cell therapies. Mech Ageing Dev. 2008;129(3):163–73.

6. Einhorn TA, Gerstenfeld LC. Fracture healing: mechanisms and interventions. Nat Rev Rheumatol. 2015;11(1):45–54.

7. Fulop T, Larbi A, Dupuis G, Le Page A, Frost EH, Cohen AA, Witkowski JM, Franceschi C. Immunosenescence and inflamm-aging as two sides of the same coin: friends or foes? Front Immunol. 2017;8:1960.

8. Cohen HJ, Pieper CF, Harris T, Rao KM, Currie MS. The association of plasma IL-6 levels with functional disability in community-dwelling elderly. J Gerontol A Biol Sci Med Sci. 1997;52(4):M201–8.

9. Bruunsgaard H, Skinhoj P, Pedersen AN, Schroll M, Pedersen BK. Ageing, tumour necrosis factor-alpha (TNF-alpha) and atherosclerosis. Clin Exp Immunol. 2000;121(2):255–60.

10. Schmidt-Bleek K, Schell H, Schulz N, Hoff P, Perka C, Buttgereit F, Volk HD, Lienau J, Duda GN. Inflammatory phase of bone healing initiates the regenerative healing cascade. Cell Tissue Res. 2012;347(3):567–73.

11. Thomas MV, Puleo DA. Infection, inflammation, and bone regeneration: a paradoxical relationship. J Dent Res. 2011;90(9):1052–61.

12. Thevaranjan N, Puchta A, Schulz C, Naidoo A, Szamosi JC, Verschoor CP, Loukov D, Schenck LP, Jury J, Foley KP, Schertzer JD, Larche MJ, Davidson DJ, et al. Age-associated microbial dysbiosis promotes intestinal permeability, systemic inflammation, and macrophage dysfunction. Cell Host Microbe. 2017;21(4):455–66.

13. Roberts JL, Golloshi M, Harding DB, Conduah M, Liu G, Drissi H. Bifidobacterium longum supplementation improves age-related delays in fracture repair. Aging Cell. 2023;22:e13786.

14. Roberts JL, Liu G, Darby TM, Fernandes LM, Diaz-Hernandez ME, Jones RM, Drissi H. Bifidobacterium adolescentis supplementation attenuates fracture-induced systemic sequelae. Biomed Pharmacother. 2020;132:110831.

15. Vester H, Huber-Lang MS, Kida Q, Scola A, van Griensven M, Gebhard F, Nussler AK, Perl M. The immune response after fracture trauma is different in old compared to young patients. Immun Ageing. 2014;11(1):20.

16. Emami AJ, Toupadakis CA, Telek SM, Fyhrie DP, Yellowley CE, Christiansen BA. Age dependence of systemic bone loss and recovery following femur fracture in mice. J Bone Miner Res. 2019;34(1):157–70.

17. Badal VD, Vaccariello ED, Murray ER, Yu KE, Knight R, Jeste DV, Nguyen TT. The Gut Microbiome, Aging, and Longevity: A Systematic Review. Nutrients. 2020;12(12):3759.

18. Fransen F, van Beek AA, Borghuis T, Aidy SE, Hugenholtz F, van der Gaast-de Jongh C, Savelkoul HFJ, De Jonge MI, Boekschoten MV, Smidt H, Faas MM, de Vos P. Aged gut microbiota contributes to systemical inflammaging after transfer to germ-free mice. Front Immunol. 2017;8:1385.

19. Cooney OD, Nagareddy PR, Murphy AJ, Lee MKS. Healthy gut, healthy bones: targeting the gut microbiome to promote bone health. Front Endocrinol. 2020;11:620466.

20. Haffner-Luntzer M, Fischer V, Ignatius A. Differences in fracture healing between female and male C57BL/6J mice. Front Physiol. 2021;12:712494.

21. Soung DY, Talebian L, Matheny CJ, Guzzo R, Speck ME, Lieberman JR, Speck NA, Drissi H. Runx1 dose-dependently regulates endochondral ossification during skeletal development and fracture healing. J Bone Miner Res. 2012;27(7):1585–97.

22. Roberts JL, Kinter CW, Drissi H. Generation and experimental outcomes of closed femoral fracture in mice. Methods Mol Biol. 2021;2221:205–22.

23. Paglia DN, Diaz-Hernandez ME, Roberts JL, Kalinowski J, Lorenzo J, Drissi H. Deletion of Runx1 in osteoclasts impairs murine fracture healing through progressive

woven bone loss and delayed cartilage remodeling. J Orthop Res. 2019;38(5):1007–15.

24. Cauley JA, Barbour KE, Harrison SL, Cloonan YK, Danielson ME, Ensrud KE, Fink HA, Orwoll ES, Boudreau R. Inflammatory markers and the risk of hip and vertebral fractures in men: the osteoporotic fractures in men (MrOS). J Bone Miner Res. 2016;31(12):2129–38.

25. Kluber P, Meurer SK, Lambertz J, Schwarz R, Zechel-Gran S, Braunschweig T, Hurka S, Domann E, Weiskirchen R. Depletion of lipocalin 2 (LCN2) in mice leads to dysbiosis and persistent colonization with segmented filamentous bacteria. Int J Mol Sci. 2021;22(23):13156.

26. Wei S, Bahl MI, Baunwall SMD, Hvas CL, Licht TR. Determining gut microbial dysbiosis: a review of applied indexes for assessment of intestinal microbiota imbalances. Appl Environ Microbiol. 2021;87(11):e00395.

27. Zura R, Mehta S, Della Rocca GJ, Steen RG. Biological risk factors for nonunion of bone fracture. JBJS Rev. 2016;4(1):e5.

28. Hebb JH, Ashley JW, McDaniel L, Lopas LA, Tobias J, Hankenson KD, Ahn J. Bone healing in an aged murine fracture model is characterized by sustained callus inflammation and decreased cell proliferation. J Orthop Res. 2018;36(1):149–58.

29. Loffler J, Sass FA, Filter S, Rose A, Ellinghaus A, Duda GN, Dienelt A. Compromised bone healing in aged rats is associated with impaired M2 macrophage function. Front Immunol. 2019;10:2443.

30. Roberts JL, Drissi H. Advances and promises of nutritional influences on natural bone repair. J Orthop Res. 2020;38(4):695–707.

31. Simsek T, Simsek HU, Canturk NZ. Response to trauma and metabolic changes: posttraumatic metabolism. Ulus Cerrahi Derg. 2014;30(3):153–9.

32. Cuthbertson D, Tilstone WJ. Metabolism during the postinjury period. Adv Clin Chem. 1969;12:1–55.

33. Slade Shantz JA, Yu YY, Andres W, Miclau T 3rd, Marcucio R. Modulation of macrophage activity during fracture repair has differential effects in young adult and elderly mice. J Orthop Trauma. 2014;28(Suppl 1):S10–4.

34. Yukata K, Xie C, Li TF, Takahata M, Hoak D, Kondabolu S, Zhang X, Awad HA, Schwarz EM, Beck CA, Jonason JH, O'Keefe RJ. Aging periosteal progenitor cells have reduced regenerative responsiveness to bone injury and to the anabolic actions of PTH 1-34 treatment. Bone. 2014;62:79–89.

35. Gibon E, Lu L, Goodman SB. Aging, inflammation, stem cells, and bone healing. Stem Cell Res Ther. 2016;7:44.

36. Hashimoto J, Yoshikawa H, Takaoka K, Shimizu N, Masuhara K, Tsuda T, Miyamoto S, Ono K. Inhibitory effects of tumor necrosis factor alpha on fracture healing in rats. Bone. 1989;10(6):453–7.

37. Glass GE, Chan JK, Freidin A, Feldmann M, Horwood NJ, Nanchahal J. TNF-alpha promotes fracture repair by augmenting the recruitment and differentiation of muscle-derived stromal cells. Proc Natl Acad Sci U S A. 2011;108(4):1585–90.

38. Yoshikawa H, Hashimoto J, Masuhara K, Takaoka K, Ono K. Inhibition by tumor necrosis factor of induction of ectopic bone formation by osteosarcoma-derived bone-inducing substance. Bone. 1988;9(6):391–6.

39. Fajardo LF, Kwan HH, Kowalski J, Prionas SD, Allison AC. Dual role of tumor necrosis factor-alpha in angiogenesis. Am J Pathol. 1992;140(3):539–44.

40. Andruszkow H, Fischer J, Sasse M, Brunnemer U, Andruszkow JH, Gansslen A, Hildebrand F, Frink M. Interleukin-6 as inflammatory marker referring to multiple organ dysfunction syndrome in severely injured children. Scand J Trauma Resusc Emerg Med. 2014;22:16.

41. Maier B, Lefering R, Lehnert M, Laurer HL, Steudel WI, Neugebauer EA, Marzi I. Early versus late onset of multiple organ failure is associated with differing patterns of plasma cytokine biomarker expression and outcome after severe trauma. Shock. 2007;28(6):668–74.

42. Ono T, Okamoto K, Nakashima T, Nitta T, Hori S, Iwakura Y, Takayanagi H. IL-17-producing γδ T cells enhance bone regeneration. Nat Commun. 2016;7:10928.

43. Dixit M, Singh KB, Prakash R, Singh D. Functional block of IL-17 cytokine promotes bone healing by augmenting FOXO1 and ATF4 activity in cortical bone defect model. Osteoporos Int. 2017;28(7):2207–20.

44. Huang H, Kim HJ, Chang EJ, Lee ZH, Hwang SJ, Kim HM, Lee Y, Kim HH. IL-17 stimulates the proliferation and differentiation of human mesenchymal stem cells: implications for bone remodeling. Cell Death Differ. 2009;16(10):1332–43.

45. Kocic J, Santibanez JF, Krstic A, Mojsilovic S, Dordevic IO, Trivanovic D, Ilic V, Bugarski D. Interleukin 17 inhibits myogenic and promotes osteogenic differentiation of C2C12 myoblasts by activating ERK1,2. Biochim Biophys Acta. 2012;1823(4):838–49.

46. Jo S, Wang SE, Lee YL, Kang S, Lee B, Han J, Sung IH, Park YS, Bae SC, Kim TH. IL-17A induces osteoblast differentiation by activating JAK2/STAT3 in ankylosing spondylitis. Arthritis Res Ther. 2018;20(1):115.

47. Noh M. Interleukin-17A increases leptin production in human bone marrow mesenchymal stem cells. Biochem Pharmacol. 2012;83(5):661–70.

48. Tan JY, Lei LH, Chen XT, Ding PH, Wu YM, Chen LL. AKT2 is involved in the IL17Amediated promotion of differentiation and calcification of murine preosteoblastic MC3T3E1 cells. Mol Med Rep. 2017;16(5):5833–40.

49. Osta B, Lavocat F, Eljaafari A, Miossec P. Effects of interleukin-17A on osteogenic differentiation of isolated human mesenchymal stem cells. Front Immunol. 2014;5:425.

50. Uluckan O, Jimenez M, Karbach S, Jeschke A, Grana O, Keller J, Busse B, Croxford AL, Finzel S, Koenders M, van den Berg W, Schinke T, Amling M, et al. Chronic skin inflammation leads to bone loss by IL-17-mediated inhibition of Wnt signaling in osteoblasts. Sci Transl Med. 2016;8(330):330ra337.

51. Shaw AT, Maeda Y, Gravallese EM. IL-17A deficiency promotes periosteal bone formation in a model of inflammatory arthritis. Arthritis Res Ther. 2016;18(1):104.

52. Tyagi AM, Srivastava K, Mansoori MN, Trivedi R, Chattopadhyay N, Singh D. Estrogen deficiency induces the differentiation of IL-17 secreting Th17 cells: a new candidate in the pathogenesis of osteoporosis. PLoS One. 2012;7(9):e44552.

53. Wang Z, Jia Y, Du F, Chen M, Dong X, Chen Y, Huang W. IL-17A Inhibits osteogenic differentiation of bone

mesenchymal stem cells via Wnt signaling pathway. Med Sci Monit. 2017;23:4095–101.

54. Kim YG, Park JW, Lee JM, Suh JY, Lee JK, Chang BS, Um HS, Kim JY, Lee Y. IL-17 inhibits osteoblast differentiation and bone regeneration in rat. Arch Oral Biol. 2014;59(9):897–905.

55. Ahmadi S, Razazan A, Nagpal R, Jain S, Wang B, Mishra SP, Wang S, Justice J, Ding J, McClain DA, Kritchevsky SB, Kitzman D, Yadav H. Metformin reduces aging-related leaky gut and improves cognitive function by beneficially modulating gut microbiome/goblet cell/mucin axis. J Gerontol A Biol Sci Med Sci. 2020;75(7):e9–e21.

56. Hsieh H, Morin J, Filliettaz C, Varada R, LaBarre S, Radi Z. Fecal lipocalin-2 as a sensitive and noninvasive biomarker in the TNBS Crohn's inflammatory bowel disease model. Toxicol Pathol. 2016;44(8):1084–94.

57. Chassaing B, Srinivasan G, Delgado MA, Young AN, Gewirtz AT, Vijay-Kumar M. Fecal lipocalin 2, a sensitive and broadly dynamic non-invasive biomarker for intestinal inflammation. PLoS One. 2012;7(9):e44328.

58. Asimakopoulou A, Weiskirchen S, Weiskirchen R. Lipocalin 2 (LCN2) Expression in hepatic malfunction and therapy. Front Physiol. 2016;7:430.

59. Langille MG, Meehan CJ, Koenig JE, Dhanani AS, Rose RA, Howlett SE, Beiko RG. Microbial shifts in the aging mouse gut. Microbiome. 2014;2(1):50.

60. Bartosch S, Fite A, Macfarlane GT, McMurdo ME. Characterization of bacterial communities in feces from healthy elderly volunteers and hospitalized elderly patients by using real-time PCR and effects of antibiotic treatment on the fecal microbiota. Appl Environ Microbiol. 2004;70(6):3575–81.

61. Claesson MJ, Jeffery IB, Conde S, Power SE, O'Connor EM, Cusack S, Harris HM, Coakley M, Lakshminarayanan B, O'Sullivan O, Fitzgerald GF, Deane J, O'Connor M, et al. Gut microbiota composition correlates with diet and health in the elderly. Nature. 2012;488(7410):178–84.

62. Claesson MJ, Cusack S, O'Sullivan O, Greene-Diniz R, de Weerd H, Flannery E, Marchesi JR, Falush D, Dinan T, Fitzgerald G, Stanton C, van Sinderen D, O'Connor M, et al. Composition, variability, and temporal stability of the intestinal microbiota of the elderly. Proc Natl Acad Sci U S A. 2011;108(Suppl 1):4586–91.

63. Mariat D, Firmesse O, Levenez F, Guimaraes V, Sokol H, Dore J, Corthier G, Furet JP. The Firmicutes/Bacteroidetes ratio of the human microbiota changes with age. BMC Microbiol. 2009;9:123.

64. Zwielehner J, Liszt K, Handschur M, Lassl C, Lapin A, Haslberger AG. Combined PCR-DGGE fingerprinting and quantitative-PCR indicates shifts in fecal population sizes and diversity of Bacteroides, bifidobacteria and Clostridium cluster IV in institutionalized elderly. Exp Gerontol. 2009;44(6-7):440–6.

65. Hoffman JD, Parikh I, Green SJ, Chlipala G, Mohney RP, Keaton M, Bauer B, Hartz AMS, Lin AL. Age drives distortion of brain metabolic, vascular and cognitive functions, and the gut microbiome. Front Aging Neurosci. 2017;9:298.

66. Wu CS, Muthyala SDV, Klemashevich C, Ufondu AU, Menon R, Chen Z, Devaraj S, Jayaraman A, Sun Y. Age-dependent remodeling of gut microbiome and host serum metabolome in mice. Aging (Albany NY). 2021;13(5):6330–45.

67. Winter SE, Baumler AJ. Why related bacterial species bloom simultaneously in the gut: principles underlying the 'Like will to like' concept. Cell Microbiol. 2014;16(2):179–84.

68. Baldelli V, Scaldaferri F, Putignani L, Del Chierico F. The role of Enterobacteriaceae in gut microbiota dysbiosis in inflammatory bowel diseases. Microorganisms. 2021;9(4):697.

69. Thongaram T, Hoeflinger JL, Chow J, Miller MJ. Prebiotic galactooligosaccharide metabolism by probiotic lactobacilli and bifidobacteria. J Agric Food Chem. 2017;65(20):4184–92.

70. Malmir H, Ejtahed HS, Soroush AR, Mortazavian AM, Fahimfar N, Ostovar A, Esmaillzadeh A, Larijani B, Hasani-Ranjbar S. Probiotics as a new regulator for bone health: a systematic review and meta-analysis. Evid Based Complement Alternat Med. 2021;2021:3582989.

71. Henrick BM, Rodriguez L, Lakshmikanth T, Pou C, Henckel E, Arzoomand A, Olin A, Wang J, Mikes J, Tan Z, Chen Y, Ehrlich AM, Bernhardsson AK, et al. Bifidobacteria-mediated immune system imprinting early in life. Cell. 2021;184(15):3884–98.

72. Miyauchi E, Ogita T, Miyamoto J, Kawamoto S, Morita H, Ohno H, Suzuki T, Tanabe S. Bifidobacterium longum alleviates dextran sulfate sodium-induced colitis by suppressing IL-17A response: involvement of intestinal epithelial costimulatory molecules. PLoS One. 2013;8(11):e79735.

73. Liwen Z, Yu W, Liang M, Kaihong X, Baojin C. A low abundance of Bifidobacterium but not Lactobacillius in the feces of Chinese children with wheezing diseases. Medicine (Baltimore). 2018;97(40):e12745.

74. Shi P, Dong W, Nian D, Chen Y, Liu X, Qu H, Li Q. Bifidobacterium alleviates guillain-barré syndrome by regulating the function of T17 cells. Int J Clin Exp Med. 2018;11(5):4779–86.

75. Liu HX, Rocha CS, Dandekar S, Wan YJ. Functional analysis of the relationship between intestinal microbiota and the expression of hepatic genes and pathways during the course of liver regeneration. J Hepatol. 2016;64(3):641–50.

76. Rampelli S, Candela M, Turroni S, Biagi E, Collino S, Franceschi C, O'Toole PW, Brigidi P. Functional metagenomic profiling of intestinal microbiome in extreme ageing. Aging (Albany NY). 2013;5(12):902–12.